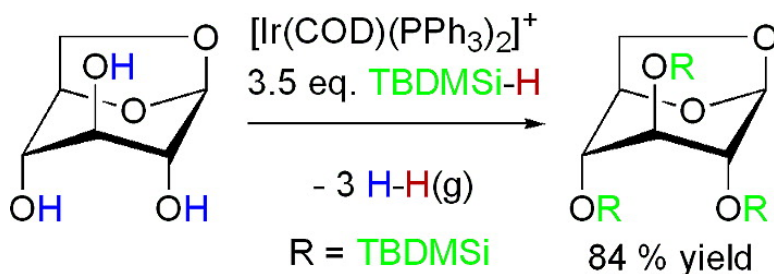


Regioselectively Trisilylated Hexopyranosides through Homogeneously Catalyzed Silane Alcoholysis

Mee-Kyung Chung, and Marcel Schlaf

J. Am. Chem. Soc., **2005**, 127 (51), 18085-18092 • DOI: 10.1021/ja056283i • Publication Date (Web): 30 November 2005

Downloaded from <http://pubs.acs.org> on March 25, 2009



More About This Article

Additional resources and features associated with this article are available within the HTML version:

- Supporting Information
- Links to the 2 articles that cite this article, as of the time of this article download
- Access to high resolution figures
- Links to articles and content related to this article
- Copyright permission to reproduce figures and/or text from this article

[View the Full Text HTML](#)

Regioselectively Trisilylated Hexopyranosides through Homogeneously Catalyzed Silane Alcoholysis

Mee-Kyung Chung and Marcel Schlaf*

Contribution from the The Guelph-Waterloo Centre for Graduate Work in Chemistry (GWC),
Department of Chemistry, University of Guelph, Guelph, Ontario, Canada N1G 2W1

Received September 12, 2005; E-mail: mschlaf@uoguelph.ca

Abstract: The iridium complex $[\text{Ir}(\text{COD})(\text{PPh}_3)_2]^+\text{SbF}_6^-$ reacts with *tert*-butyldimethylsilane in DMA to form $[\text{IrH}_2(\text{Sol})_2(\text{PPh}_3)_2]^+\text{SbF}_6^-$, which is an active catalyst for the regioselective di- and trisilylation of a series of representative methyl hexopyranosides, β -1,6-anhydrohexopyranosides and 1,3,5-*O*-methylidene inositol. The corresponding 2,3,6- and 2,4,6-silylated glycosides are obtained in a separable mixture of 47–89% (2,3,6-isomers) and 9–25% (2,4,6-isomers) yield in a single-pot reaction. The 2,4-disilylated derivatives of mannosan, galactosan, and 1,3,5-*O*-methylidene inositol as well as persilylated levoglucosan are accessible in >85% yield by this method. The homogeneous nature of the catalysts is a prerequisite for the effective di-/trisilylation, as nanoparticle colloid catalysts generated in situ from $\text{Pd}_2(\text{dba})_3$ (~1.5 nm average particle size) or $\text{Ru}_2\text{Cl}_5(\text{MeCN})_7$ (~0.65 nm average particle size) result in only low yields.

Introduction

Silyl ethers find widespread application as protecting groups in synthetic carbohydrate chemistry.¹ The most common method for their introduction into sugars is the reaction of one or several hydroxyl functions in the sugar with a trialkylsilyl chloride or a mixed alkyl/arylsilyl chloride in the presence of a base, such as pyridine or imidazole. Due to its relative stability against acid or base and ease of removal with tetrabutylammonium fluoride, *tert*-butyldimethylsilyl chloride (TBDMSi-Cl) is often the silylation reagent of choice for this purpose.^{2–4} Recently, we developed a new synthetic methodology to introduce this silyl ether protecting group into a series of simple glycosides of common monosaccharides.⁵ The method is based on the silane alcoholysis reaction, catalyzed by in situ generated Pd nanoparticle colloids and using *tert*-butyldimethylsilane (TBDMSiH) or Ph_3SiH as the silanes in *N,N*-dimethylacetamide (DMA) solvent. The methodology gives convenient access to the 3,6-silylated methyl or phenyl glycopyranosides as the dominant product rather than the 2,6-silylated methyl or phenyl glycopyranosides typically obtained by the silyl chloride method.⁶

To be used directly as potential glycosyl acceptors or for further transformation of a single hydroxyl function, an additional protection of one of the remaining free hydroxyl functions at C-2, C-3, or C-4 in the either the 2,6- or 3,6-disilylated sugars is desirable. To avoid additional protection

steps and to mediate a triple direct one-step selective protection, we therefore decided to change the catalyst in our methodology and evaluated the catalytic activity of various homogeneous catalysts for silane alcoholysis reactions with sugars, based on the hypothesis that homogeneous catalysts might be more active and thus be able to mediate a triple silylation on these substrates in a single reaction.

The results presented here show that the complex rhodium and iridium ionic salts $[\text{M}(\text{COD})(\text{PPh}_3)_2]^+\text{SbF}_6^-$ (M = Ir, Rh; COD = 1,5-cyclooctadiene) form effective catalysts, generating the targeted trisilylated sugars regioselectively in one step. Applying these catalysts to a series of methyl pyranosides, 1,6- β -D-anhydro-pyranoses and 1,3,5-*O*-methylidene-*myo*-inositol, tri- or disilylated derivatives with only one free hydroxyl function are obtained in moderate to excellent yield. For the majority of the sugar substrates investigated, the isolated yields of the trisilylated derivatives substantially exceed those of any previously known routes. The regioselectivity and mechanism of the $[\text{M}(\text{COD})(\text{PPh}_3)_2]^+\text{SbF}_6^-$ (M = Ir, Rh)-catalyzed silane alcoholysis reactions have also been investigated in direct comparison to the *classical* silyl chloride method.

Choice of Solvent, Silane, and Sugar Substrates. Following the same the rationale and building on the results of our earlier study,⁵ the highly polar yet unreactive solvent *N,N*-dimethylacetamide (DMA) and TBDMSiH as the silane were again employed. For sugar substrates, we again focused our study on the methyl glycosides of glucose, mannose, galactose as well as the conformationally locked sugar derivatives 1,6-anhydro- β -D-glucose (levoglucosan), 1,6-anhydro- β -D-mannose (mannosan), 1,6-anhydro- β -D-galactose (galactosan), and 1,3,5-*O*-methylidene-*myo*-inositol. For reference throughout this paper, the structures and numbering scheme for all sugar substrates investigated are shown in Chart 1.

(1) Collins, P.; Ferrier, R. *Monosaccharides*; John Wiley & Sons: Toronto, 1995.

(2) Chen, M.-Y.; Lu, K.-C.; Lee, A. S.-Y.; Lin, C.-C. *Tetrahedron Lett.* **2002**, *43*, 2777–2780.

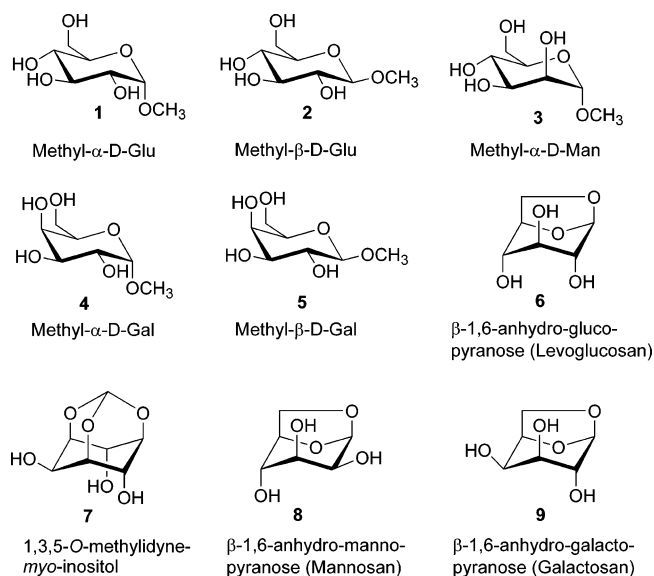
(3) Corey, E. J.; Venkateswarlu, A. *J. Am. Chem. Soc.* **1972**, *94*, 6190–6191.

(4) Kraska, B.; Klemmer, A.; Hagedorn, H. *Carbohydr. Res.* **1974**, *36*, 398–403.

(5) Chung, M.-K.; Orlova, G.; Goddard, J. D.; Schlaf, M.; Harris, R.; Beveridge, T. J.; White, G.; Hallett, F. R. *J. Am. Chem. Soc.* **2002**, *124*, 10508–10518.

(6) Halmos, T.; Montserrat, R.; Filippi, J.; Anonakis, K. *Carbohydr. Res.* **1987**, *170*, 57–69.

Chart 1



Numbering scheme:

- # a: Monosilylated in position 6 with TBDMSi
b: 2,6-disilylated with TBDMSi
c: 3,6-disilylated with TBDMSi
d: 4,6-disilylated with TBDMSi
e: 2,4-disilylated with TBDMSi for Ino
f: 2,3,6-trisilylated with TBDMSi
g: 2,4,6-trisilylated with TBDMSi
h: 3,4,6-trisilylated with TBDMSi
i: 2,3-disilylated with TBDMSi for anhydro-pyranose
j: 2,4-disilylated with TBDMSi for anhydro-pyranose
k: 3,4-disilylated with TBDMSi for anhydro-pyranose
l: 2,3,4-fully silylated with TBDMSi for anhydro-pyranose

Results and Discussion

Catalyst Evaluation and Selection. To identify catalysts capable of effecting a one-step trisilylation of monosaccharides, a series of test reactions were carried out using methyl- α -D-glucopyranoside as the common model substrate. All reactions were carried out by dissolving the model substrate (1.0 mmol) and 3.5 equiv of TBDMSiH in DMA (6.0 mL) and adding a catalyst precursor (4.0 mol % metal content with respect to sugar) at ambient temperature and subsequently heating the reaction mixture to 70 °C. The completion of the reaction was indicated by the cessation of hydrogen gas evolution. The reaction mixture was then concentrated in vacuo and treated with activated charcoal and filtered to remove the catalyst. The crude product was subjected to flash column chromatography in order to separate its respective isomers. (See Experimental Section and Supporting Information for details on the chromatography conditions for all sugars investigated.)

Ten catalysts were selected to study their effect on silane alcoholysis of methyl- α -D-glucopyranoside (Table 1). $\text{Ru}_2(\mu\text{-Cl})_2\text{Cl}_2(\text{CO})_4(\text{PMe}_3)_2$,⁷ $\text{RuCl}_2(\text{CO})_2(\text{PMe}_3)_2$ (*cis,cis,trans*-),⁸ $\text{RhCl}(\text{PPh}_3)_3$,^{9–11} RhCl_3 (triphos),¹² $\text{Ru}_2\text{Cl}_3(\text{MeCN})_7$,^{13,14} and $[\text{Ir}(\text{COD})\text{Cl}]_2$ ¹⁵

were selected based on the results of the model reactions using the ethylene glycol–triethylsilane system in an earlier study.⁷ These catalysts are readily available either commercially or by simple syntheses. In addition, all except $\text{RuCl}_2(\text{CO})_2(\text{PMe}_3)_2$ (*cis,cis,trans*-) had previously shown high catalytic activities in model systems with an excess amount of silane.⁷ The hydrosilylation catalyst $[\text{Rh}(\text{COD})\text{Cl}]_2$ ^{16–19} was also employed to compare the catalytic activity to that of $[\text{Ir}(\text{COD})\text{Cl}]_2$. The palladium complex, $\text{Pd}_2(\text{dba})_3$ ($\text{dba} = \text{C}_6\text{H}_5\text{CH}=\text{CHCOCH}=\text{CHC}_6\text{H}_5$),²⁰ was employed instead of PdCl_2 and $\text{Pd}(\text{OAc})_2$ since the latter had shown low activities toward trisilylation reactions as reported earlier.⁵ The palladium catalyst, $\text{Pd}_2(\text{dba})_3$, was anticipated to show a higher activity for trisilylation due to the smaller particle size of Pd(0) nanoparticles in situ derived from $\text{Pd}_2(\text{dba})_3$ in situ during the reaction. The identity of the true catalytically active species generated from $\text{Pd}_2(\text{dba})_3$ will be described below. The catalytic activities of $[\text{Ir}(\text{COD})(\text{PPh}_3)_2]^+\text{SbF}_6^-$,²¹ the precursor of Crabtree's catalyst, and the analogue $[\text{Rh}(\text{COD})(\text{PPh}_3)_2]^+\text{SbF}_6^-$ for the silane alcoholysis had to date been unknown, while, like Wilkinson's catalyst, both are known to be active in the hydrogenation of olefins. Therefore, with the assumption that it might be possible to obtain high catalytic activities toward silane alcoholysis, both salts $[\text{Ir}(\text{COD})(\text{PPh}_3)_2]^+\text{SbF}_6^-$ and $[\text{Rh}(\text{COD})(\text{PPh}_3)_2]^+\text{SbF}_6^-$ were also employed even though they had previously not been tested against the ethylene glycol model system.⁷ The rhodium complex $[\text{Rh}(\text{COD})(\text{PPh}_3)_2]^+\text{SbF}_6^-$ was obtained by the same synthetic procedure as the iridium complex reported by Osborn et al., except that reaction temperature was ambient temperature instead of 60 °C.²²

The results of the reactions on methyl- α -D-glucopyranosides with those catalysts are summarized in Table 1. Since the reactions are performed with 3.5 equiv of TBDMSiH, disilylated or trisilylated sugars are the main products depending on the catalytic activity of the catalyst used. Any monosilylated sugars formed were not included in the results. As is evident from Table 1, among all catalysts, the $[\text{M}(\text{COD})(\text{PPh}_3)_2]^+\text{SbF}_6^-$ ($\text{M} = \text{Rh}, \text{Ir}$) complexes are the only ones to generate high yields of trisilylated sugars. Therefore, these cationic complexes were selected for trisilylation reactions for the series of sugar substrates presented below. One of the ruthenium catalysts, *cis,cis,trans*- $\text{RuCl}_2(\text{CO})_2(\text{PMe}_3)_2$, showed no reactivity, consistent with the results of the model reactions using the ethylene glycol–triethylsilane system.⁷ For the other catalysts, the disilylated sugars are the dominant products, and among them, the 3,6-disilylated isomer is the main product in yields of ~40–60%. The disilylated product distributions thus resemble those obtained from Pd(0) nanoparticle colloid catalyzed reactions,⁵ which in turn are complementary to those achieved through the classical silyl chloride/imidazole method.⁶ These results suggest that metal-mediated catalytic systems prefer the silylation of hydroxyl function at C-3 (OH-3) among secondary hydroxyl

- (7) Chung, M.-K.; Ferguson, G.; Robertson, V.; Schlaf, M. *Can. J. Chem.* **2001**, *79*, 949–957.
(8) Oehmichen, U.; Singer, H. *J. Organomet. Chem.* **1983**, *243*, 199–204.
(9) Corriu, R. J.; Moreau, J. J. E. *J. Chem. Soc., Chem. Commun.* **1973**, 38–39.
(10) Corriu, R. J. P.; Moreau, J. J. E. *J. Organomet. Chem.* **1976**, *114*, 135–144.
(11) Ojima, I.; Kogure, T.; Nihonyanagi, M.; Kono, H.; Inaba, S. *Chem. Lett.* **1973**, 501–504.
(12) Ott, J.; Venanzi, L. M. *J. Organomet. Chem.* **1985**, *291*, 889–100.
(13) Jansen, A.; Gorls, H.; Pitter, S. *Organometallics* **2000**, *19*, 135–138.
(14) Jansen, A.; Pitter, S. *J. Mol. Catal. A* **2004**, *217*, 41–45.

- (15) Blackburn, S. N.; Haszeldien, R. N.; Parish, R. V. *J. Organomet. Chem.* **1980**, *192*, 329–338.
(16) Iovel, I.; Popelis, J.; Gaukhman, A.; Lukevics, E. *J. Organomet. Chem.* **1998**, *559*, 123–130.
(17) Reyes, C.; Prock, A.; Giering, W. P. *Organometallics* **2002**, *21*, 546–554.
(18) Reyes, C.; Prock, A.; Giering, W. P. *J. Organomet. Chem.* **2003**, *671*, 13–26.
(19) Takeuchi, R.; Tanouchi, N. *Chem. Commun.* **1993**, 1319–1320.
(20) Murata, M.; Suzuki, K.; Watanabe, S.; Masuda, Y. *J. Org. Chem.* **1997**, *62*, 8569–8571.
(21) Luo, X.-L.; Crabtree, R. H. *J. Am. Chem. Soc.* **1989**, *111*, 2527–2535.
(22) Schrock, R. R.; Osborn, J. A. *J. Am. Chem. Soc.* **1971**, *93*, 2397–2407.

Table 1. Silane Alcoholysis Reactions of Methyl- α -D-glucopyranoside with Various Catalysts (4.0 mol % with respect to sugar content and 3.5 equiv of TBDMSiH at 70 °C in DMA)

entry	catalyst	yield of trisilylated derivatives (%) ^a	yield of disilylated derivatives (%) ^a			total yield of tri- and disilylated derivatives (%) ^a
			2,6	3,6	4,6	
1	Ru ₂ (μ -Cl) ₂ Cl ₂ (CO) ₄ (P(CH ₃) ₃) ₂	5	21	58	6	90 ^d
2	RuCl ₂ (CO) ₂ (P(CH ₃) ₃) ₂ (<i>cis,cis,trans</i>)					
3	RhCl(PPh ₃) ₃	19	15	63	3	100
4	RhCl ₃ (triphos)	5	18	47	8	78 ^d
5	[Ir(COD)Cl] ₂	43		46		89 ^d
6	[Rh(COD)Cl] ₂	15	17	61	5	98
7	[Ir(COD)(PPh ₃) ₂] ⁺ SbF ₆ ⁻	98				98
8	[Rh(COD)(PPh ₃) ₂] ⁺ SbF ₆ ⁻	87		9		96
9	Ru ₂ Cl ₅ (MeCN) ₇ ^b	12	27	44	5	88 ^d
10	Pd ₂ (dba) ₃ ^c	5	18	47	8	78 ^d

^a Isolated yields after overnight reaction (15 h) and cessation of H₂(g) evolution. Isomer distributions are listed in Table 3. ^b Actual catalytic species are in situ generated Ru(0) nanoparticle colloids. ^c Actual catalytic species are in situ formed Pd(0) nanoparticle colloids. ^d The remainder of silylated derivatives are monosilylated derivatives and were not isolated.

Table 2. Results of the Characterization of the Palladium Colloids and the Ruthenium Colloids by TEM

	Catalyst Precursor	
	Pd ₂ (dba) ₃	Ru ₂ Cl ₅ (CH ₃ CN) ₇
No. of particles sampled	100	95
temperature (°C)	25	25
mean size (nm)	1.49	0.62
ESD	0.31	0.15
min size (nm)	0.86	0.08
max size (nm)	2.15	0.93

functions of methyl- α -D-glucopyranoside. The increased reactivity at OH-3 is not well understood, but may be due to either the feasibility of steric interactions between sugar substrates and metal catalysts or electronic properties of the combined sugar substrate–metal catalyst systems.

Nanoparticle Structure of the Catalysts Derived from Pd₂(dba)₃ and Ru₂Cl₅(MeCN)₇. The Ru₂Cl₅(MeCN)₇ and Pd₂(dba)₃ complexes have been shown to give active catalysts for silane alcoholysis and hydrosilylation reactions, respectively.^{13,20} For the Pd₂(dba)₃ complex, we found that the addition of sugar in DMA to the purple DMA solution of TBDMSiH and Pd₂(dba)₃ generated a black solution of homogeneous appearance very similar to those obtained from PdX₂ (X = Cl⁻, OAc⁻) and TBDMSiH in DMA by us⁵ and in less polar solvents by others.^{23–25} For the Ru₂Cl₅(MeCN)₇ complex, we also observed that the addition of TBDMSiH to a yellow suspension of Ru₂Cl₅(MeCN)₇ in DMA resulted in a black solution. On the basis of these observations, we suspected the identities of the actual catalytic species may be Pd(0) and Ru(0) nanoparticle colloids in each case and characterized them both by transmission electron microscopy (TEM).

Table 2 summarizes the results of the TEM analyses of representative colloids from both Ru₂Cl₅(MeCN)₇ at 25 °C and Pd₂(dba)₃ generated at 25 °C in the presence of a 40-fold excess of TBDMSiH. For the latter, the addition of a 30-fold excess of anhydrous MeOH was required to generate Pd(0) colloids. Without the addition of sugar or simple alcohols, the purple DMA solution of Pd₂(dba)₃ and TBDMSiH does not turn black

even after 1 day. Presumably, the MeOH displaces the dba from the Pd(0) in a coordination equilibrium. Once the dba is displaced, a coagulation of Pd(0) can occur. Once the nanoparticles of Pd(0) formed, they are stabilized by a coating of either TBDMSi, TBDMSi–SiTBDM—possibly generated by a Pd(0)-mediated dehydrogenative coupling reaction of two molecules of TBDMSiH—or by TBDMSiOMe obtained by the silylation reaction of MeOH.²⁶ The particle size distribution was reproducible within the error ranges indicated in the Table 2. TEM images of in situ formed Pd(0) and Ru(0) nanoparticle colloids are shown in Figure 1, and the particle size distributions of the catalysts are illustrated by the histograms in Figure 2. For both catalysts, a total of ~100 particles was measured. Compared to Pd(0) nanoparticles obtained from PdCl₂ and Pd(OAc)₂,⁵ smaller nanoparticles with a more narrow size distribution were obtained for both Ru₂Cl₅(MeCN)₇ and Pd₂(dba)₃.

Regioselective Trisilylation of Methyl Glycopyranosides with the [M(COD)(PPh₃)₂]⁺SbF₆⁻ (M = Ir, Rh)-Derived Catalysts. Table 3 summarizes the results of the silane alcoholysis reactions of the series of methyl glycopyranosides **1–5** (see Chart 1) and compares them to those (given in parentheses) obtained by the classical silyl chloride method.⁶ Each trisilylated isomer was identified by ¹H COSY, ¹³C JMOD, ¹H/¹³C HSQC, and ¹H/¹³C HMBC NMR spectroscopy (see Supporting Information for an exhaustive collection of NMR data and spectra images).

The notable feature of the silane alcoholysis reaction using [M(COD)(PPh₃)₂]⁺SbF₆⁻ (M = Rh, Ir) as the catalyst is that the yields of trisilylated sugars are much higher than those achieved by the classical TBDMSiCl/base method. In particular, for the glucose and galactose derivatives **1**, **2**, **4**, and **5**, the 2,3,6-trisilylated isomers were produced in synthetically useful yields with the iridium catalyst. The 2,4,6-trisilylated isomer (**2g**) derived from the glucose derivatives **2** and 3,4,6-trisilylated isomer (**3h**) derived from the mannose derivatives **3** are all new and might be potentially very useful for synthesizing new types of oligosaccharides even though each yield is comparatively low. The silane alcoholysis reactions also show a distinct regioselectivity in the product distributions. For all reactions using the iridium catalyst, 2,3,6-trisilylated isomers are the main product, and as disilylated products, only 3,6-isomers were obtained. For most reactions with the rhodium catalyst, the 2,3,6-isomers are still the major product, while the yields are lower

(23) Chauhan, B. P. S.; Rathore, J. S.; Chaihan, M.; Krawicz, A. *J. Am. Chem. Soc.* **2003**, *125*, 2876–2877.

(24) Chauhan, B. P. S.; Rathore, J. S.; Gillokhani, N. *Appl. Organomet. Chem.* **2005**, *19*, 542–550.

(25) Fowley, L. A.; Michos, D.; Luo, X.-L.; Crabtree, R. H. *Tetrahedron Lett.* **1993**, *34*, 3075.

(26) Chung, M. K.; Schlaf, M. *J. Am. Chem. Soc.* **2004**, *126*, 7386–7392.

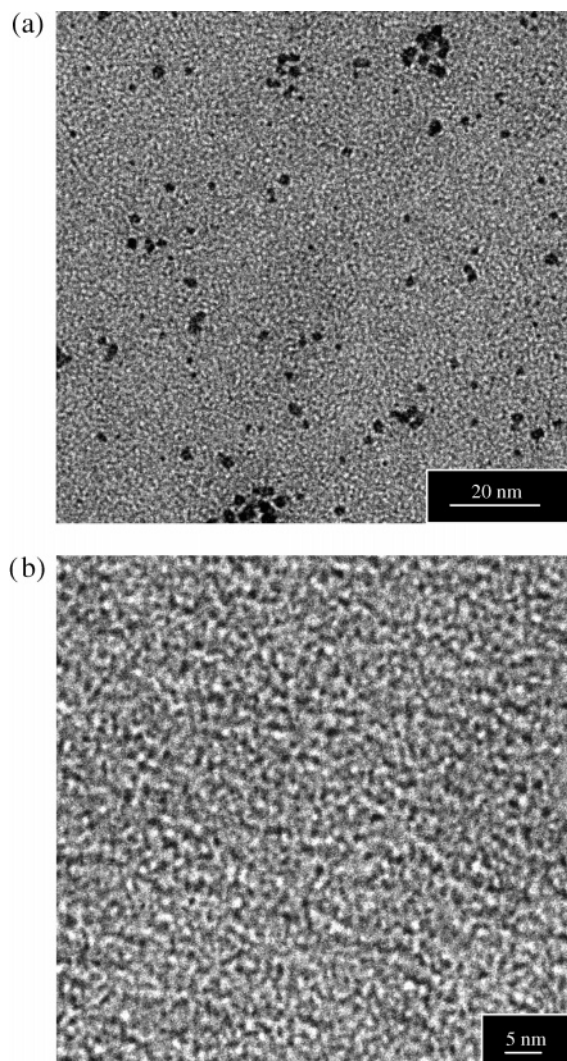


Figure 1. (a) TEM image of a colloid formed $\text{Pd}_2(\text{dba})_3$ at 25 °C. (b) TEM image of a colloid formed $\text{Ru}_2\text{Cl}_5(\text{MeCN})_7$ at 25 °C.

than those obtained by reactions with the iridium catalyst, but as with the iridium catalyst, only 3,6-isomers were produced. With the classical $\text{TBDMSiCl}/\text{base}$ method, the differences in yields between 2,4,6- and 2,3,6- isomers are—with the exception of the galactose substrate **4**—less pronounced ($\leq 13\%$ in each case).

Considering the reactions with the iridium catalyst in more detail, it emerges that when the stereochemical relation between the anomeric methoxy group and the hydroxyl function at C-2 (OH-2) in sugar molecules is changed from *cis*- to *trans*-, that is, from the α -substrate to the β -substrate, the yields of the 2,3,6-isomers decrease while those of 2,4,6-isomers are almost the same or show a slight increase (entry 1 \rightarrow 2 and entry 4 \rightarrow 5, Table 3). No statement on the influence of the anomeric configuration on the regioselectivity can be made for the mannose substrate **3** (entry 3, Table 3), as the β -anomer is not readily available and was therefore not included in the study. If the stereochemistry of the hydroxyl function at C-4 (OH-4) is changed from an equatorial to an axial position, that is, the relationship between OH-4 and OH-3 changes from *trans*- to *cis*-, the yields of the 2,3,6-isomers increase while those of 2,4,6-isomers decrease slightly or are unchanged (entry 1 \rightarrow 4 and entry 2 \rightarrow 5, Table 3). It appears that when OH-2 is axial OH-4

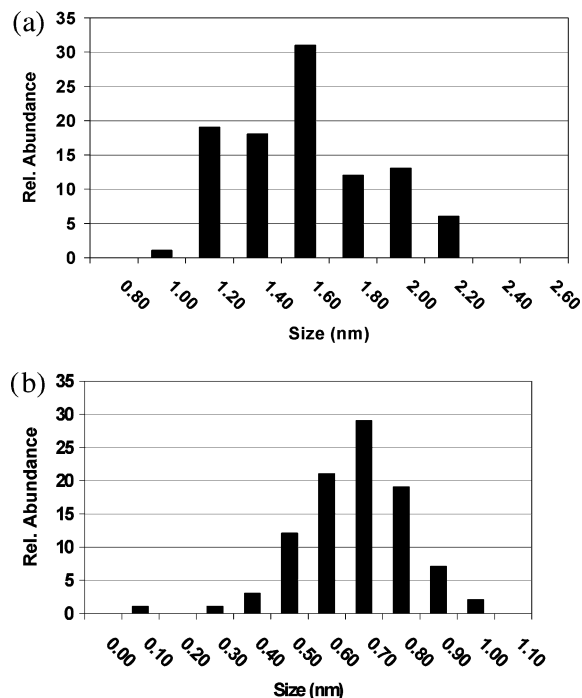


Figure 2. (a) The particle size distributions obtained by TEM in a Pd(0) colloid generated from $\text{Pd}_2(\text{dba})_3/\text{TBDMSiH}/\text{MeOH}$ at 25 °C in DMA. (b) The particle size distributions obtained by TEM in a Ru(0) colloid generated from $\text{Ru}_2\text{Cl}_5(\text{MeCN})_7/\text{TBDMSiH}$ at 25 °C in DMA (resolution is 0.1 nm because of the narrow particle size distribution).

becomes more reactive to generate 3,4,6-isomers as well as 2,4,6-isomers. For reactions using the rhodium catalyst, these trends still emerge, albeit somewhat less pronounced.

In all reactions, there are no unsilylated starting glycosides left, and the 3,6-disilylated isomers, which are initially silylated in the most reactive primary position 6^{5,6} and only subsequently in position 3, appear in most cases as the single byproduct. The trisilylated sugars are therefore produced in a series of stepwise silylations, starting with monosilylation in position 6, subsequent disilylation in position 2, 3, or 4, and final trisilylation on one of the remaining free hydroxyl functions. The product distributions observed for the trisilylated derivatives should therefore be a direct function of the product distributions of the disilylated derivatives.

Attempted Rationalization of the Observed Isomer Distributions: Synthesis of Trisilylated Sugars from Disilylated Precursors. To test the hypothesis stated above, first, the product distributions of the disilylated derivatives obtained from a silane alcoholysis reaction catalyzed by the iridium complex were determined for the methyl-D-glycopyranosides **1–5**. The disilylation reactions were empirically optimized by variation of temperature and amount of silane employed and compared with the results achieved earlier with in situ generated Pd(0) nanoparticle colloids and the $\text{TBDMSiCl}/\text{base}$ method.^{5,6} Lowering the amount of silane used from 3.5 to 2.3 equiv relative to the sugar and the temperature from 45 °C to ambient yields the disilylated isomer mixtures as the main products.

Table 4 summarizes the results of these experiments. No or only low yields of the 4,6-disilylated derivatives were formed for all substrates. For glucose and galactose substrates, the regioselectivity bias of 3,6 over 2,6 almost doubles from α - to β -substrates, contrary to results obtained with the Pd(0) nanoparticle colloids.⁵

Table 3. Isolated Yields for the Regioselective Trisilylation of Methylhexopyranosides with the [M(COD)(PPh₃)₂]⁺SbF₆⁻ (M = Ir, Rh) (4.0 mol %)/TBDMSiH (3.5 equiv) System at 70 °C^a

entry	sugar substrate	catalyst	yield of disilylated derivatives (%)	yield of trisilylated derivatives (%)			yield of tetrasilylated derivatives (%)	total yield of silylated sugars (%)
				2,3,6	2,4,6	3,4,6	2,3,4,6	
1	methyl- α -D-Glu (1)	Ir	9	73	25	<1	<1	98
				Rh	58	25	2	<1
2	methyl- β -D-Glu (2)	Ir	18	(-)	(29)	(42)	(-)	(79)
				Rh	44	17	38	1
3	methyl- α -D-Man (3)	Ir	9	(8)	(-)	(-)	(38)	(70)
				Rh	23	22	24	19
4	methyl- α -D-Gal (4)	Ir	(28)	(21)	(30)	(-)	(5)	(84)
				Rh	2	59	32	2
5	methyl- β -D-Gal (5)	Ir	(33)	(57)	(6)	(-)	(-)	(96)
				Rh	64	25	8	<2
			(20)	(39)	(38)	(-)	(-)	(97)

^a Results for TBDMSiCl (4.3 equiv)/base method in brackets are taken from Halmos et al.⁶ ^b Not determined.

Table 4. Isolated Yields for the Regioselective Disilylation of Methylhexopyranosides with the [Ir(COD)(PPh₃)₂]⁺SbF₆⁻ (3.0 mol %)/TBDMSiH (2.3 equiv) System and in Comparison with Those Achieved by Pd(0) Nanoparticle Colloids^a

entry	sugar substrate	catalyst	temp (°C)	yield of disilylated derivatives (%)			yield of trisilylated derivatives (%)	total yield of silylated sugars (%)
				2,6	3,6	4,6		
1	methyl- α -D-Glu (1)	Ir	45	19	58	6	3	86
			Pd ⁰	rt	18	63	5	3
2	methyl- β -D-Glu (2)	Ir	rt	(70)	(11)	(-)	(9)	(92)
			Pd ⁰	rt	12	69	2	9
3	methyl- α -D-Man (3)	Ir	rt	19	62	6	3	90
			Pd ⁰	rt	(20)	(20)	(-)	(-)
4	methyl- α -D-Gal (4)	Ir	rt	11	83	4	4	98
			Pd ⁰	rt	9	62	1	7
5	methyl- β -D-Gal (5)	Ir	45	(50)	(33)	(5)	(9)	(97)
			Pd ⁰	rt	38	41	7	6
			rt	36	39	6	6	81
			rt	(66)	(21)	(-)	(10)	(97)
			rt	29	53	16	16	98
			rt	30	37	2	2	69
			rt	(35)	(43)	(-)	(8)	(86)

^a Results for TBDMSiCl (2.3 equiv)/base method in brackets are taken from Halmos et al.⁶

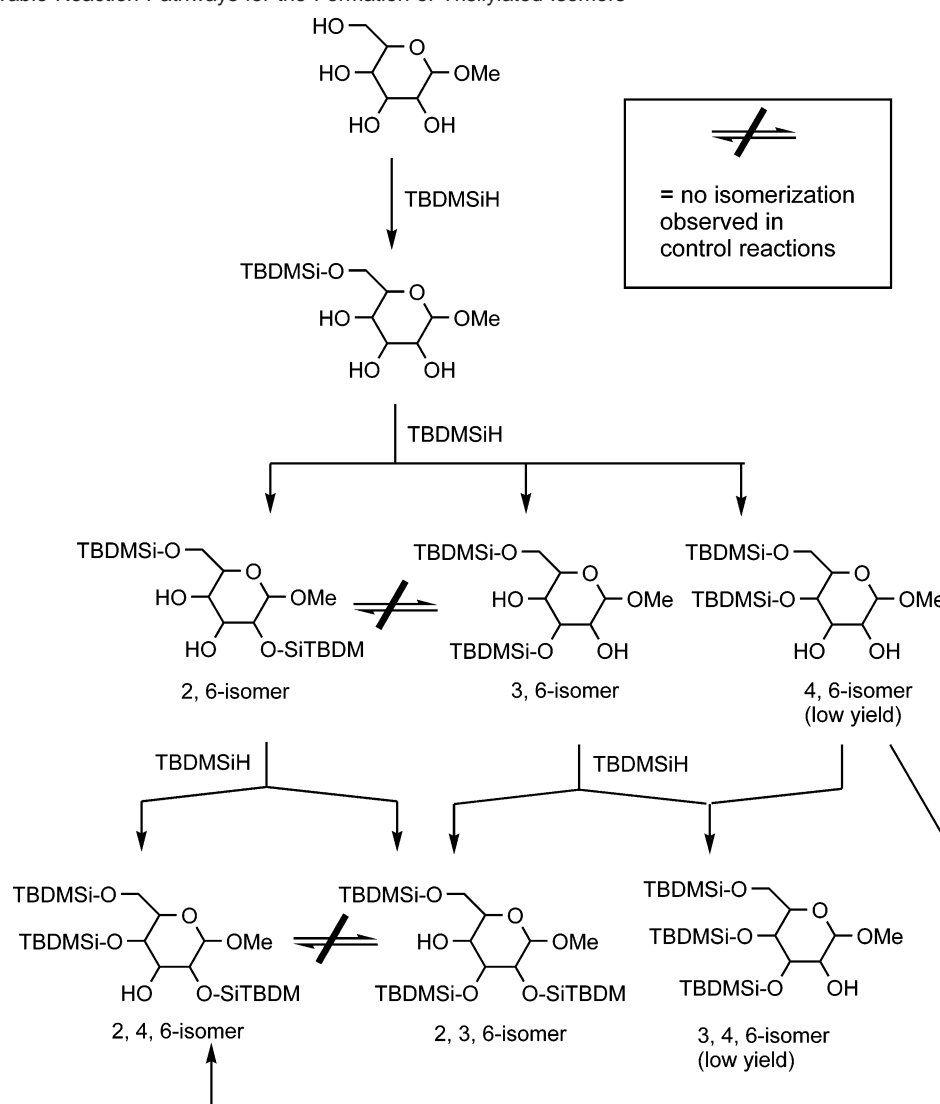
However, overall, the 3,6-disilylated pyranosides are still the main products, similar to the results obtained with the Pd(0) nanoparticle colloids/TBDMSiH system. This is noteworthy as one set of results is obtained by a homogeneous catalyst system and the other by a heterogeneous catalyst system.

The correlation of the product distribution from the trisilylation to that of the disilylation reactions using the iridium catalyst was analyzed (first row of each entry in Tables 3 and 4). In the disilylation reaction, 3,6-isomers are obtained in increased yields for β -sugar substrates (Table 4), but in the trisilylation reaction, the 2,3,6-isomers that may be derived from the 3,6-isomers are produced in relatively lower yields for the corresponding sugar substrates (Table 3). For example, for the α -galactose substrate, the trisilylated 2,3,6-isomer is the major (first row of entry 4, Table 3), while the yield of the disilylated 3,6-isomer is almost same as that of the 2,6-isomer (first row of entry 4, Table 4). Therefore, with these results, it is not immediately evident whether the product distributions of the trisilylated derivatives are a direct and simple function of the product distributions of the disilylated derivatives.

As is can be seen from Scheme 1, each of the trisilylated isomers is accessible by two routes: the 2,4,6-isomer may be

generated from either the 2,6- or the 4,6-isomer, the 2,3,6-isomer from either the 2,6- or the 3,6-isomer, and the 3,4,6-isomer from either the 3,6- or the 4,6-isomer. Previously, under the classical TBDMSiCl/imidazole reaction condition, silyl group migrations between *cis*-related hydroxyl functions were reported by Halmos et al.⁶ That is, appreciable migrations occur between 2,6- and 3,6-isomers in the mannose substrate and the 3 \rightarrow 4 migration in 2,3,6-trisilylated isomers of α - and β -galactose substrates under the reaction condition of the classical method.

If these migrations occur under the silane alcoholysis reaction conditions, some of the trisilylated isomers could result from more than the two routes shown in Scheme 1. For example, the 2,4,6-isomer of the mannose substrate may be produced from the 2,6-isomer itself or from a silylation of 2,6-isomer resulting from a the 3 \rightarrow 2 silyl group migration of the 3,6-isomer initially formed. In both galactose substrates, the 2,4,6-isomer may also be obtained either from the 4,6-isomers resulting from a 3 \rightarrow 4 silyl group migration of the 3,6-isomers or directly through the 3 \rightarrow 4 silyl group migration of the 2,3,6-trisilylated isomers with two routes as stated above. To exclude these possibilities, we carried out control experiments examining potential silyl group migrations between 3,6- and 2,6-isomers in the mannose

Scheme 1. Conceivable Reaction Pathways for the Formation of Trisilylated Isomers**Table 5.** Yields for the Regioselective Trisilylation of 2,6-Disilylated Hexopyranosides with the $[\text{Ir}(\text{COD})(\text{PPh}_3)_2]^+\text{SbF}_6^-$ (4.0 mol %)/TBDMSiH (1.7 equiv) System at 70 °C^a

entry	sugar substrate	yield of trisilylated derivatives (%)		yield of tetrasilylated derivatives (%)
		2,3,6	2,4,6	2,3,4,6
1	2,6-Di-TBDMSi -methyl- α -D-Glu (1b)	44	56	0
2	2,6-Di-TBDMSi -methyl- β -D-Glu (2b)	22	77	1
3	2,6-Di-TBDMSi -methyl- α -D-Man (3b)	6	85	9
4	2,6-Di-TBDMSi -methyl- α -D-Gal (4b)	88	12	0
5	2,6-Di-TBDMSi -methyl- β -D-Gal (5b)	45	55	0

^a Yields were determined by the ratio of integration of anomeric protons in ¹H NMR spectroscopic data. There is no starting material left.

substrate and between 2,3,6- and 2,4,6-isomers in both galactose substrates under the actual silane alcoholysis reaction conditions. These control experiments showed no isomerizations due to the silyl group migrations for all tested sugar substrates.

In light of these results and hypothesizing that the nature of the disilylated isomer predetermines the type of trisilylated isomer formed, further silylation reactions of the series of 2,6-isomers to the possible trisilylated isomers were investigated under the same reaction conditions as the original trisilylation reactions (see Table 3), but employing only 1.7 equiv of silane. As the 3,4,6-isomer is—with the exception of substrate **3**—only

formed in comparatively low yield in the original trisilylation reactions, the alternative investigation of the product distribution arising from additional silylation of the 3,6-isomer is less attractive. The reactions of the 4,6-isomer were not considered as the obtained yields of this isomer in the disilylation product distributions are either very low ($\leq 6\%$) or not at all.

Table 5 shows the results of the silylation reactions of the 2,6-disilylated sugar substrates. In all cases, both the 2,3,6- and 2,4,6-isomers are generated. In the glucose and the galactose derivatives **1b** and **5b**, 2,3,6- and 2,4,6-isomers are generated in a ratio of almost 1:1, which suggests that the 2,3,6-isomer

Table 6. Isolated Yields for the Regioselective Trisilylation of Conformationally Locked Sugar Derivatives with the $[M(\text{COD})(\text{PPh}_3)_2]^+\text{SbF}_6^-$ ($M = \text{Ir}, \text{Rh}$) (4.0 mol %)/TBDMSiH (2.3 equiv) System at 70 °C^a

entry	sugar substrate	catalyst	disilylated derivatives (%)			fully silylated derivatives (%)	total silylated derivatives (%)
			2,4	2,3	3,4		
1	1,6-anhydro- β -D-Glu (6)	Ir ^b	15			84	99
		Ir	42	12 ^b		42	96
		Rh	48	22	6	11	87
2	1,6-anhydro- β -D-Man (8)	Ir	86	<2 ^c		5	93
		Rh	79	<2 ^c		3	84
3	1,6-anhydro- β -D-Gal (9)	Ir	87	4	<1	6	98
		Rh	62	22	3	6	97
4	1,3,5- <i>O</i> -methylidene- <i>myo</i> -inositol (7)	Ir	91				91
		Rh	88				88
			(47)				(47)

^a Results for TBDMSiCl (4.3 equiv)/base method in brackets are taken from Halmos et al.⁶ ^b TBDMSiH (3.5 equiv). ^c Mixtures of 2,3- and 3,4-silylated derivatives.

may be generated from both the 2,6- and 3,6-isomers and may be a main product regardless of the amount of 2,6- and 3,6-isomers in disilylation product distribution. For the α -galactose substrate **4b**, the 2,3,6-isomer can also be the main product regardless of the amount of each disilylated isomers since the 2,6-isomer is mostly transformed into the 2,3,6-isomer. In the other glucose and the mannose substrates **2b** and **3b**, however, mainly the 2,4,6-isomer is obtained. This suggests that to produce either the 2,3,6- or the combination of 2,3,6- and 3,4,6-isomers as a majority the amount of 3,6-isomer should be higher than that of the 2,6-isomer in disilylation product distribution of the above sugar substrates **2b** and **3b**.

An overall comparison of the data in Table 3 with those of the stepwise silylation in Tables 4 and 5 gives some insight into the sequence of the silylation reactions and reveals that the overall silylation patterns observed are indeed most likely the result of an in situ stepwise disilylation followed by an additional silylation to give the trisilylated products. This process is well modeled by the separation of the two silylations steps. Considering, for example, in the silylation of compound **2b** (entry 2 in Tables 3–5), it appears that the overall isomer distribution, which is dominated by the 2,3,6-isomer, is a composite of an initial preferential 3,6-silylation (3,6:2,6 ratio of approximately 6:1) and the subsequent trisilylation step, which shows various preference to hydroxyl functions dependent on the nature of disilylated isomers.

Homogeneously Catalyzed Regioselective Silylation of Conformationally Locked Sugar Derivatives. Using $[M(\text{COD})(\text{PPh}_3)_2]^+\text{SbF}_6^-$ ($M = \text{Ir}, \text{Rh}$) as the catalyst, we also applied our method to the conformationally locked sugar derivatives, levoglucosan (**6**), mannosan (**8**), galactosan (**9**), and 1,3,5-*O*-methylidene-*myo*-inositol (**7**). Table 6 summarizes the results of these experiments.

All compounds in Table 6 are new except the 2,4-disilylated and fully silylated inositols of entry 4. In all cases, the 2,4-disilylated sugars are the main products as disilylated derivatives, and this substitution pattern is probably due to steric interactions. For levoglucosan, the method using the iridium catalyst gives fully silylated 2,3,4-trisilylated levoglucosan in synthetically useful yield (~84%). This fully silylated levoglucosan may be synthetically valuable in the preparation of the glucose having free hydroxyl functions in C-6 and the anomeric carbon C-1 with all others protected. This substitution pattern might be very useful in the synthesis of oligosaccharides.

Nature of the Homogeneous Catalysts Employed. The cationic species $[\text{Ir}(\text{COD})(\text{PPh}_3)_2]^+$ had previously been shown to be an active catalyst for olefin hydrogenation.^{27,28} In contrast, its activity for silane alcoholysis has to date not been reported. As is evident from the results presented above, it is a highly active catalyst for the silane alcoholysis reaction capable of effecting the trisilylation of sugars. During the silane alcoholysis reaction, the direct addition of the iridium complex to the reaction mixture consisting of the sugar substrates and TBDMSiH in DMA leads to a color change of the solution from red to pale yellow within 10 min, after which begins the immediate evolution of hydrogen gas, the byproduct of the silane alcoholysis reaction. From this observation, we suspected that the actual active species of catalytic reactions is not $[\text{Ir}(\text{COD})(\text{PPh}_3)_2]^+\text{SbF}_6^-$, but rather the same $[\text{IrH}_2(\text{COD})(\text{PPh}_3)_2]^+\text{SbF}_6^-$ or $[\text{IrH}_2(\text{Sol})_2(\text{PPh}_3)_2]^+\text{SbF}_6^-$ dihydride complex that had previously been shown to be an active silane alcoholysis catalyst by Luo and Crabtree.²¹ It is known that the red solution of $[\text{Ir}(\text{COD})(\text{PPh}_3)_2]^+\text{SbF}_6^-$ in CH_2Cl_2 decolorizes upon admission of hydrogen to the reaction mixture to generate the cationic species $[\text{IrH}_2(\text{COD})(\text{PPh}_3)_2]^+$. It had also been shown by Luo and Crabtree that the hydrogenation of $[\text{Ir}(\text{COD})(\text{PPh}_3)_2]^+\text{SbF}_6^-$ at low temperature leads to the hydrogenative loss of the COD ligand in the form of cyclooctane to produce the active catalyst $[\text{IrH}_2(\text{Sol})_2(\text{PPh}_3)_2]^+\text{SbF}_6^-$, where “Sol” is a coordinating solvent such as methanol or THF or acetone. On the basis of these studies, it is logical to postulate that, in our reaction conditions, the complex would also be transformed into $[\text{IrH}_2(\text{Sol})_2(\text{PPh}_3)_2]^+\text{SbF}_6^-$ by in situ generated H_2 gas originating from the silane. To test this hypothesis, we carried out several NMR scale experiments under inert atmosphere. Addition of an excess TBDMSiH (ca. 10 equiv) to the complex in DMF-*d*₇ (the commercially available deuterated solvent most closely resembling DMA) at 70 °C resulted in the formation of several hydride species, as indicated by the NMR spectrum upfield to 0 ppm (vs TMS). Also, no identifiable cyclooctadiene (COD) vinyl proton resonance remains in the spectrum. Among several hydride resonances, the most abundant hydride resonance corresponds to that of $[\text{IrH}_2(\text{Sol})_2(\text{PPh}_3)_2]^+\text{SbF}_6^-$ in DMF-*d*₇ (δ -27.8 ppm; $^2J(\text{P}-\text{H}) = 16.3$ Hz). In the ³¹P NMR spectroscopic data, this species shows a multiplet of δ 28.3 ppm,

(27) Crabtree, R. H.; Demou, P. C.; Eden, D.; Mihelcic, J. M.; Parnell, C. A.; Quirk, J. M.; Morris, G. E. *J. Am. Chem. Soc.* **1982**, *104*, 6994–7001.

(28) Crabtree, R. H.; Felkin, H.; Morris, G. E. *J. Organomet. Chem.* **1977**, *141*, 205–215.

which is very similar to a triplet at δ 28.1 ppm in $[\text{IrH}_2(\text{Sol})_2(\text{PPh}_3)_2]^+\text{SbF}_6^-$. These resonance patterns indicate that during the silane alcoholysis reactions the cationic complex is indeed transformed into Crabtree's catalyst, $[\text{IrH}_2(\text{Sol})_2(\text{PPh}_3)_2]^+\text{SbF}_6^-$, or at least into a species with very similar structural features. Clearly, other hydride ligand containing species, possibly incorporating η^2 -coordinated silane and/or solvent, are present, but an elucidation of the precise composition of each species was beyond the scope of our present goals.

For the analogous rhodium species, $[\text{Rh}(\text{COD})(\text{PPh}_3)_2]^+\text{SbF}_6^-$, a similar NMR scale experiment was carried out, leading to a brown solution that showed no hydride species but according to the results presented above still shows catalytic activity. Again, no vinyl resonance for a COD ligand was detected. The ^{31}P NMR spectroscopic data indicate the presence of a multitude of species, suggesting that no well defined catalytically active complex is formed, but possibly rhodium(0) is present with the intriguing possibility that a nanostructured heterogeneous catalyst similar to those described above may have been formed.

Conclusion

The $[\text{M}(\text{COD})(\text{PPh}_3)_2]^+\text{SbF}_6^-$ ($\text{M} = \text{Ir}, \text{Rh}$) cationic complexes are highly active catalysts for the regioselective silylation of simple glycopyranosides with TBDMSiH by silane alcoholysis. In particular, the 2,3,6- and 2,4,6-trisilylated derivatives, which are generally difficult to obtain by the *classical* silyl chloride method, are conveniently available in synthetically useful yields by the new method. For $\text{M} = \text{Ir}$, the actual catalytically active species formed in situ is the previously described $[\text{IrH}_2(\text{Sol})_2(\text{PPh}_3)_2]^+\text{SbF}_6^-$ complex.

Experimental Section

General. All synthetic experiments were performed under a dry argon atmosphere using standard Schlenk-line techniques. Sample solutions for Transmission Electron Microscopy (TEM) were prepared inside an inert-gas drybox under argon atmosphere.

Electron microscopy was carried out on a LEO 912AB operating at 100 kV with a liquid nitrogen anticontaminator in place. Digital images were collected using a $1\text{K} \times 1\text{K}$ PROSCAN CCD camera and processed using the measurement software in the SIS EsiVision program. Both negatively stained (using 2% w/v uranyl acetate) and unstained samples were imaged for measurement comparison. All figures in this paper are of unstained samples, so that the region of electron density in each particle is attributed to the palladium.

NMR spectra were recorded at 400 MHz. Isomer assignments of the silylated sugar species were made on the basis of 2D COSY, HSQC, and HMBC spectra (see Supporting Information details). Sugar

substrates, *t*-BuMe₂SiH (TBDMSi-H), and metal salts were purchased from commercial sources and used as received. *N,N*-Dimethylacetamide (DMA) was dried by vacuum distillation from BaO and subsequently stored over activated 4 Å molecular sieves. Flash column chromatography was performed on wet-packed silica gel (60 μm) at 1 psi static pressure set by a break-through valve at the column head. Details for the chromatographic separations of the individual sugars are given in the Supporting Information.

General Procedure for the Catalytic Tri- or Disilylation of Sugar Substrates. A DMA (6 mL) solution of the substrate (1.0 mmol) and TBDMSiH (2.3–4.3 equiv, depending on the experiment performed) was prepared in a one-neck round-bottom Schlenk flask fitted with a Schlenk stopcock. The catalyst was added as a solid, the apparatus connected to a gas bubbler, and the reaction stirred at the indicated reaction temperature until hydrogen gas evolution stopped (10–24 h) and TLC indicated completion of the reaction. DMA was removed by rotary evaporation at 45 °C under full oil-pump vacuum, and the catalysts were removed by treatment with active charcoal. Flash column chromatography of the residue with various solvent systems yields the silylated substrates as well as separated isomers. See Supporting Information for detailed spectroscopic and chromatography data on the individual compounds.

Preparation of Samples for TEM. TBDMSiH (1.2 mmol) was added to Pd₂(dba)₃ (0.03 mmol) or Ru₂^{II/III}(CH₃CN)₇ (0.03 mmol) dissolved in dry DMA (6 mL). For Pd₂(dba)₃, dried MeOH (1.0 mmol) is added to generate colloids. After stirring for 2 h, 3 mL of the sample solution was collected. The black solution was then removed from the glovebox and the specimen mounted on Formvar/carbon 200-mesh copper grids by floating the grid face down on the sample suspension for 30 s and blotting off the excess on a filter paper. To stain the samples, they were next floated on a drop of 2% w/v uranyl acetate for 10 s and then blotted.

Acknowledgment. Funding was provided by the Natural Science and Engineering Research Council of Canada (NSERC), the Canadian Foundation for Innovation (CFI), the Ontario Innovation Trust Fund (OIT), and the University of Guelph. Transmission Electron Microscopy (TEM) was performed by Robert Harris in the NSERC Guelph Regional STEM Facility, which is partially funded by an NSERC Major Facilities Access Grant.

Supporting Information Available: Comprehensive collection of 400 MHz ¹H and ¹³C NMR data (COSY, HSQC, and HMBC) for all silylated products with images of all spectra, peak assignments, and conditions for chromatographic isolation (63 pages, print/PDF). This material is available free of charge via the Internet at <http://pubs.acs.org>.

JA056283I